ApJL
Preprint typeset using LaTeX style emulateapj v. 7/8/03

arXiv:astro-ph/0307516v1 30 Jul 2003

DAMPED LYα GAS METALLICITIES AT REDSHIFTS $Z = 0.9 - 2.0$ FROM SDSS SPECTRA[1]

Daniel B. Nestor[2], Sandhya M. Rao[2], David A. Turnshek[2], and Daniel Vanden Berk[2]
Department of Physics & Astronomy, University of Pittsburgh, Pittsburgh, PA 15260
ApJL, accepted (submitted 04/22/03)

ABSTRACT

Using Sloan Digital Sky Survey (SDSS) early data release spectra, we have identified 370 Mg II absorption systems with Mg II λ2796 rest equivalent widths ≥ 1 Å and redshifts $z = 0.9 - 2.2$. From our previous and ongoing HST UV spectroscopic studies, we estimate that the mean neutral hydrogen column density of a system selected in this manner is $N_{HI} = 3.6 \pm 1.3 \times 10^{20}$ atoms cm^{-2}, which corresponds to the damped Lyα (DLA) regime. We have formed high signal-to-noise ratio composite spectra using 223 of these systems with $z = 0.9 - 2.0$ in order to study the strength of the Zn II and Cr II absorption lines corresponding to this mean neutral hydrogen column density. After making a correction for missed DLAs, overall we find that [Zn/H] $= -1.13 \pm 0.19$. We find [Cr/Zn] $= -0.45 \pm 0.13$, which indicates that $\approx 65\%$ of the Cr is depleted on to grains, but this does not correct for the missed DLAs. We have also derived Zn and Cr abundances in two kinematic regimes, and within each regime we consider two redshift intervals. We find trends which indicate that metallicities are higher in the composites where the absorption has larger velocity spreads as measured by Mg II λ2796 rest equivalent width. Larger velocity spreads may correspond to deeper gravitational potential wells which represent more massive and chemically evolved structures, and/or regions associated with winds from starbursting galaxies, also leading to kinematically broad structures of chemically enriched gas. Within the large velocity spread regime, we find that at lower redshifts the Zn metallicity is larger and more Cr is depleted on to grains.

Subject headings: galaxies: abundances — galaxies: evolution — galaxies: formation — nucleosynthesis — quasars: absorption lines

1. INTRODUCTION

Over a decade ago Pettini and collaborators presented the first in a series of studies aimed at deriving metal abundances for the neutral-gas-phase component of the Universe at high redshift (see Pettini et al. 1999 and references therein). In their initial studies they relied on medium-resolution spectroscopy of the Zn II $\lambda\lambda$2026,2062, and Cr II $\lambda\lambda$2056,2062,2066 absorption lines in QSO damped Lyα systems (DLAs). Measurements of metals in DLAs with $N_{HI} \geq 2 \times 10^{20}$ atoms cm^{-2} are appropriate for studies of the cosmic neutral-gas-phase metallicity because these systems trace the bulk of the neutral hydrogen gas mass of the Universe out to at least redshift $z \approx 3.5$ (see Storrie-Lombardi & Wolfe 2000, Rao & Turnshek 2000, hereafter RT2000, and references therein). It was realized that measurements of the Zn II and Cr II lines using medium-resolution spectra would likely be sufficient to consider the problem because the lines would be unsaturated even in DLAs.

However, selection effects and small number statistics continue to be important concerns in these studies. For example, the presence of dust in a subset of absorbers would dim the corresponding background QSOs, causing a bias against finding absorbers with high dust content. Moreover, while a column density-weighted determination of the cosmic metallicity is the most relevant measurement for tracking the overall chemical evolution of the neutral gas, this leads to a result mostly dominated by a few of the highest N_{HI} systems. Since individual absorbers have a range of metallicities, the uncertainty introduced by the small number of very high N_{HI} absorbers studied to date is a problem.

Instead of measuring individual QSO absorption-line systems, we take the approach of using composite spectra here, which leads to preliminary measurements of the DLA gas metallicity of the Universe at moderate redshift. We derive the composites from Sloan Digital Sky Survey (SDSS; York et al. 2000) early data release (EDR; Stoughton et al. 2002) QSO spectra (Schneider et al. 2002), which individually show evidence for high-N_{HI} absorption based on their Mg II absorption-line properties. By using these composite spectra, the worries related to small number statistics can be mitigated. We have used 223 absorption-line systems in the redshift interval $0.9 \leq z \leq 2.0$ to make composites in this initial study, representing a total integrated neutral hydrogen column density of $N_{HI}^{tot} \approx 8 \times 10^{22}$ atoms cm^{-2}. This exceeds corresponding numbers for previously studied individual systems: 42 systems over the redshift interval $0.4 < z < 3.5$ with $N_{HI}^{tot} \approx 4 \times 10^{22}$ atoms cm^{-2} (Pettini et al. 1999; Prochaska & Wolfe 1999; Molaro et al. 2000; Ge, Bechtold, & Kulkarni 2001).

2. ANALYSIS

2.1. *Sample Definition*

Using Hubble Space Telescope (HST) UV spectroscopy, RT2000 showed that strong intervening Mg II−Fe II absorption-line systems identified in QSO spectra characteristically have very high neutral hydrogen column density gas (generally $10^{19} < N_{HI} < 10^{22}$ atoms cm^{-2}). Many are DLAs with $N_{HI} \geq 2 \times 10^{20}$

[1] Based on data obtained in the Sloan Digital Sky Survey and by the Hubble Space Telescope, operated by STScI-AURA, for NASA.
[2] email: dbn@phyast.pitt.edu, rao@everest.phyast.pitt.edu, turnshek@pitt.edu, danvb@phyast.pitt.edu

atoms cm^{-2}. RT2000 showed that $\approx 95\%$ of these DLAs can be identified by selecting systems which have a Mg II λ2796 rest equivalent width (REW) $W_0^{\lambda 2796} > 0.5$ Å *and* Fe II λ2600 REW $W_0^{\lambda 2600} > 0.5$ Å. We have used these results to establish criteria for selecting high-N_{HI} systems in the past. Here we use a slightly revised criterion ($W_0^{\lambda 2796} \geq 1.0$ Å) to obtain a sample of 370 high-N_{HI} systems. It is straightforward to select absorption-line systems above this threshhold using SDSS spectra.[3] Recognizing weaker systems is also possible, but with greater incompleteness due to signal-to-noise considerations. In Nestor et al. (2003, in preparation) we will present the findings of a survey for Mg II $\lambda\lambda$2796,2802 absorption-line systems in SDSS QSO spectra. The results will establish the incidence of Mg II systems as a function of REW and also include measurements of Fe II λ2600 and Mg I λ2852, when available. The details of selecting systems (e.g., continuum fitting, equivalent width measurements, completeness) will be discussed there. It should be emphasized that our selection method basically amounts to a kinematic, as opposed to a metallicity-based, criterion. This is because the Mg II λ2796 absorption lines are on the saturated part of the curve of growth, so their REWs are essentially measures of velocity spread rather than column density.

2.2. *Forming and Measuring the Composite Spectra*

The 370 absorbers in our sample were found in 3683 SDSS EDR spectra. To form composites we continuum-normalized each spectrum (and error array) and wavelength-shifted them into the absorber rest frame. To accomplish this, a spectrum was first rebinned on a finer subpixel grid, with subpixels having one-fifth the size of an original pixel; this minimized data smoothing due to rebinning. We then used visual inspection to eliminate 70 spectra that suffered from abnormalities or poor signal-to-noise in the Zn II−Cr II region of interest. In principle, the remaining 300 spectra would all be valuable for forming composites. However, one of the goals of our analysis is to make an accurate measurement of the Zn II λ2026 absorption line, and in SDSS medium-resolution spectra this line is potentially blended with the low-oscillator-strength Mg I λ2026 absorption line. Therefore, in this initial study, we decided to estimate the contribution of Mg I λ2026 to the blend by only using spectra that also had data on the higher-oscillator-strength (but generally unsaturated) Mg I λ2852 absorption line. This resulted in the elimination of 77 more systems for which Mg II λ2852 was unavailable. We then experimented with different methods for forming composites and found that inverse variance-weighting produced the highest signal-to-noise ratio composites, so we adopted results produced by this method since there is no known correlation between N_{HI} and spectrum signal-to-noise ratio. Other methods (e.g., straight averaging) would have produced somewhat lower signal-to-noise ratio composites. We note that, if QSO dimming due to the presence of dust and, therefore, high metal content, is significant, we would be underestimating the mean metallicity, as our weighting method favors brighter QSOs.

[3] We note that our composite spectra indicate that $W_0^{\lambda 2796}$ is ≈ 1.9 times larger than $W_0^{\lambda 2600}$. Thus, we are generally consistent with the criterion that $W_0^{\lambda 2600} > 0.5$ Å.

The composite spectrum in the Zn II−Cr II region derived from the entire sample of 223 absorbers is shown in the left panel of Figure 1. The right panel of Figure 1 shows other composites formed by roughly dividing the sample into quarters while keeping the variance approximately the same. These subsamples correspond to Mg II absorbers with low REW ($1.0 \leq W_0^{\lambda 2796} < 1.3$ Å) and high REW ($W_0^{\lambda 2796} \geq 1.3$ Å), and at lower redshift ($0.9 \leq z < 1.35$) and higher redshift ($1.35 \leq z \leq 2.0$) within the total sample. This subdivision leads to some important results (§3 and §4). Measurements of the absorption lines in the Zn II−Cr II region in the five composites shown in Figure 1 are reported in Table 1, along with the characteristic properties that define the total sample and four subsamples.

2.3. *The Mean N_{HI} of the Sample*

To estimate the mean neutral hydrogen column density of the absorber sample, we have measured N_{HI} (when available) for every known Mg II system with $W_0^{\lambda 2796} \geq 1$ Å, i.e., 24 systems studied by RT2000 and 51 new systems from ongoing HST UV spectroscopy of the Lyα absorption line in strong Mg II systems (Rao et al. 2003, in preparation). These 75 systems have neutral hydrogen column densities in the range $5 \times 10^{18} < N_{HI} < 7 \times 10^{21}$ atoms cm^{-2}, and their mean neutral hydrogen column density is $<N_{HI}> = 3.6 \pm 1.3 \times 10^{20}$ atoms cm^{-2}, which we take to be the mean neutral hydrogen column density of our sample. There is no indication that the $<N_{HI}>$ values for the four subsamples are different from that determined for the entire sample.

However, the REW regime considered (§2.1) does not represent a census of all H I in the Universe over the studied redshift interval, nor does it represent all DLAs with $N_{HI} \geq 2 \times 10^{20}$ atoms cm^{-2}. RT2000 estimated that 5% of DLAs are missed using their selection criterion and the results of Nestor et al. (2002) indicate that about half of the DLAs are missed by excluding $0.5 < W_0^{\lambda 2796} < 1.0$ Å systems from a composite spectrum. Our HST spectroscopy suggests that Mg II systems in this REW range have mean neutral hydrogen column density $<N_{HI}> = 2.7 \pm 1.2 \times 10^{20}$ atoms cm^{-2}. This is 25% smaller than the mean neutral hydrogen column density for higher REW Mg II systems, but statistically equivalent given the measurement errors. These effects need to be accounted for when deriving the *cosmic* neutral-gas-phase metallicity of DLAs (§3).

3. MEASUREMENTS AND ABUNDANCE RESULTS

The basis for using the Zn II and Cr II absorption lines for element abundance determinations stems from the fact that these lines are unsaturated. This can be verified through high-resolution studies (e.g., Prochaska & Wolfe 1999). Although there has been some discussion of the importance of ionization corrections for metal abundance determinations in DLAs (e.g., Howk & Sembach 1999), we will not consider this since it is an issue that needs further study and ionization corrections have not been made when reporting DLA metal abundances in the literature. However, it is generally agreed that the bulk of the Zn and Cr is singly ionized in the DLA neutral regions. Thus, we assume that a determination of [Zn$^+$/H^0] is equivalent to [Zn/H] and a determination of [Cr$^+$/Zn$^+$] is equivalent to [Cr/Zn].

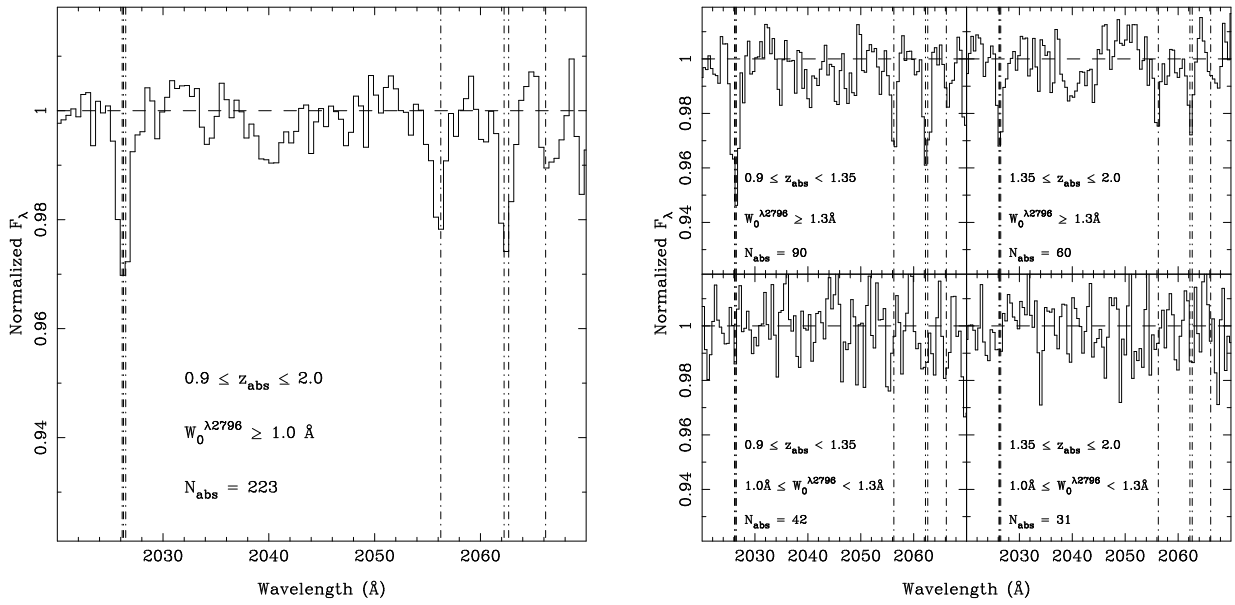

FIG. 1.— **Left:** Composite spectrum in the rest frame Zn II-Cr II region derived from 223 SDSS QSO spectra. The dash-dotted lines indicate the rest frame locations of the Zn II, Cr II, and Mg I lines (Table 1). **Right:** Composite spectra for four subsamples of the total sample divided according to redshift and Mg II λ2796 REW. Notice the presence of stronger lines (indicating more chemically evolved structures) in the larger REW (i.e. larger velocity spread) subsamples, the stronger Zn II (indicating increased metallicity) at lower redshift, and the stronger Cr II relative to Zn II (indicating less dust) at higher redshift.

TABLE 1. RESULTS FROM COMPOSITE SPECTRA MEASUREMENTS

Property	Full Sample	Low-z High-REW Subsample	High-z High-REW Subsample	Low-z Low-REW Subsample	High-z Low-REW Subsample	Cosmic DLA Gas
Number of Absorbers	223	90	60	42	31	···
Mg IIλ2796 REW (Å)	$\geq$ 1.0	$\geq$1.3	$\geq$1.3	1.0−1.3	1.0−1.3	>0
Redshift (z) Interval	0.9−2.0	0.9−1.35	1.35−2.0	0.9−1.35	1.35−2.0	0.9−2.0
Zn IIλ2026bl[1] REW (mÅ)	33.6 (5.0)	70.2 (9.3)	29.4 (7.7)	0.1 (10.6)	6.5 (11.3)	···
Mg Iλ2026bl[1] REW (mÅ)	10.2 (0.2)	13.7 (0.3)	10.9 (0.3)	5.6 (0.4)	4.0 (0.5)	···
Cr IIλ2056 REW (mÅ)	31.1 (5.1)	41.7 (7.7)	32.2 (8.1)	6.2 (10.3)	6.5 (11.4)	···
Cr IIλ2062bl[2] REW (mÅ)	23.2 (3.8)	31.2 (5.8)	24.1 (6.0)	4.6 (7.7)	4.8 (8.5)	···
Zn IIλ2062bl[2] REW (mÅ)	12.3 (6.2)	26.6 (10.3)	6.2 (9.5)	12.4 (12.9)	6.1 (14.3)	···
Cr IIλ2066 REW (mÅ)	13.0 (4.5)	19.2 (8.3)	9.8 (16.0)	21.5 (10.6)	2.5 (8.0)	···
[Zn/H][3,4]	−0.88 (0.19)	−0.56 (0.19)	−0.94 (0.21)	<-1.08	<-1.05	−1.13 (0.19)
[Cr/Zn][4]	−0.45 (0.13)	−0.64 (0.13)	−0.38 (0.18)	···	···	···
mean SDSS g mag	18.8 (0.6)	18.8 (0.5)	18.8 (0.6)	18.8 (0.6)	18.8 (0.7)	···
mean SDSS r mag	18.7 (0.5)	18.7 (0.5)	18.6 (0.6)	18.6 (0.5)	18.8 (0.6)	···

NOTE. — (1) The feature at λ2026 is a blend due to Zn II, Mg I, and a very weak Cr II line. As measured in the composite spectra, the Mg I λ2026 REW was taken to be 32.0 times smaller than the measured REW of Mg II λ2852 and the Cr II λ2026 REW was taken to be 23.0 times smaller than the measured REW of Cr IIλ2056. The remaining absorption was attributed to be due to Zn II λ2026. In a few individual QSO spectra, comparison of the strength of Mg I λ2852 to that of Mg II $\lambda\lambda$2796,2803 suggests that Mg I λ2852 may be approaching saturation, which implies that the strength of the Mg I λ2852 line may be <32.0 times the strength of Mg I λ2026. We mention this as a precaution which we will neglect for now. (2) The feature at λ2062 is a blend due to Cr II and Zn II. The REW of Cr II λ2062 was taken to be 0.50 times the measured and summed REWs of Cr II λ2056 and Cr II λ2066, or 0.75 times the measured REW of Cr II λ2056, depending on which one resulted in smaller propagated errors. The remaining absorption was then attributed to be due to Zn II λ2062. (3) When upper limits (2σ) on metallicities are reported, they represent those that apply for the quoted $W_0^{\lambda2796}$ limit or interval. Since this does not include 100% of the DLA gas (§2.3), a correction is made (§3) to derive results on the cosmic DLA gas metallicity, which is reported in the last column of this table. (4) The following oscillator strengths are adopted: $f=0.4890$ for Zn II λ2026.14, $f=0.2560$ for Zn II λ2062.66, $f=0.00471$ for Cr II λ2026.27, $f=0.105$ for Cr II λ2056.25, $f=0.0780$ for Cr II λ2062.23, $f=0.0515$ for Cr II λ2066.16, $f=0.1120$ for Mg I λ2026.48, and $f=1.8100$ for Mg I λ2852.96. See kingpin.ucsd.edu/∼hiresdla/ for details and references. Metal abundances are relative to the solar values of Grevesse & Sauval (1998).

The notes to Table 1 provide information on the method we use to deduce metal abundances, but two clarifications should be made. First, the $W_0^{\lambda2796}\geq1.0$ Å composite over the studied redshift interval does not sample all of the DLA gas. By excluding $W_0^{\lambda2796}<1.0$ Å systems, $\approx45\%$ of the DLA gas is likely to be excluded from the composite (§2.3). Second, the subsample composites with $1.0\leq W_0^{\lambda2796}<1.3$ Å show no detectable

metallicity (Table 1), suggesting that the missed DLA gas has negligible metallicity. Thus, to derive the cosmic DLA gas metallicity, we must reduce the derived metallicity in the full composite sample by a factor of ≈ 1.8. Overall we then find that [Zn/H] $= -1.13 \pm 0.19$ in DLAs, or $7.4 \pm 1.1\%$ solar. The result for Cr, which does not correct for the missed DLAs, is [Cr/Zn] $= -0.45 \pm 0.13$, indicating that $\approx 65\%$ of the Cr is depleted on to grains.

We also find that trends are present. The derived metallicities are highest in the subsamples with the largest REWs, which correspond to those with the largest velocity spreads (Table 1). Within the high-REW regime, the Zn metallicity is larger and [Cr/Zn] is smaller in the lower redshift composite. These results are equivalent to column-density-weighted determinations of cosmic neutral-gas-phase metallicities in DLAs. Our findings are consistent with and directly comparable to the results of Pettini et al. (1999) and, more recently, the results summarized by Turnshek et al. (2003).

The statistical error on $<N_{HI}>$ is 36% (0.16 dex). Thus, since the measured errors on REWs in the total sample and in the two high-REW subsamples are smaller, this error dominates the uncertainties in [Zn/H] determinations. With the aide of future HST UV spectroscopy of high-N_{HI} systems, this error may be reduced. The statistical errors in [Cr/Zn] determinations are smaller since $<N_{HI}>$ does not enter into the determinations. Recall that, within the redshift and REW intervals under study, there is at present no evidence that $<N_{HI}>$ is correlated with redshift or REW. However, if such a correlation were present, it would give rise to a systematic error requiring additional analysis to remove. In all cases the errors quoted are statistical errors propagated from REW and/or $<N_{HI}>$ measurement errors.

4. CONCLUSIONS AND DISCUSSION

We have derived cosmic DLA gas Zn and Cr abundances in two Mg II REW intervals which correspond to high and low velocity spread regimes. Within each of these kinematic regimes we have considered low-redshift ($0.9 \leq z < 1.35$) and high-redshift ($1.35 \leq z \leq 2.0$) intervals. We find that:

(1) At redshifts $0.9 \leq z \leq 2.0$, after correcting for missed DLAs, we find that the overall [Zn/H] $= -1.13 \pm 0.19$ ($\approx 7.4\%$ solar). We find [Cr/Zn] $= -0.45 \pm 0.13$ ($\approx 65\%$ of the Cr is depleted), but this does not correct for the missed DLAs.

(2) According to Savage & Sembach (1996), [Cr/Zn] values in the Milky Way Galaxy are typically -0.5 (halo), -0.8 (disk+halo), -1.1 (warm disk), and -2.1 (cool disk). Thus, while our measured value of [Cr/Zn] provides evidence for significant depletion of Cr on to dust grains, the effect is not nearly as large as in the Galactic ISM. It is of interest to assess the affect of this dust in the high-REW subsamples at low and high redshift since they exhibit the highest metallicities. For the adopted $<N_{HI}>$ of our sample ($\approx 3.6 \times 10^{20}$ atoms cm^{-2}), this amount of dust in the absorber rest frame would give rise to mean values of $<A_V^{absorber}>= 0.07$ mag for the low-redshift subsample ($<z>$=1.15, [Zn/H]$= -0.56$, [Cr/Zn]$= -0.64$) and $<A_V^{absorber}>= 0.02$ mag for the high-redshift subsample ($<z>$=1.53, [Zn/H]$= -0.94$, [Cr/Zn]$= -0.38$). This is largely independent of the nature of the dust, i.e., Galactic-like, LMC-like, or SMC-like. Individual high-Mg II-REW absorbers would undoubtedly exhibit a reasonable spread of $A_V^{absorber}$ values around these mean values, and typically the low-Mg II-REW absorbers would give rise to little extinction. For a high REW absorber at the mean redshifts of the low and high redshift subsamples, the mean V-band extinctions in the observer frame would be $<A_V^{observed}>= 0.16$ mag and $<A_V^{observed}>= 0.06$ mag, respectively. These results provide some indication of the importance of selection effects caused by dust, but the possible exclusion of extremely dusty absorbers due to dimming of background QSOs is still an open issue.

(3) There are clear trends in the composite spectra which indicate that metallicities are higher in absorption systems with larger velocity spreads (i.e., in the high-Mg II-REW absorbers). Moreover, among the high-Mg II-REW absorbers, both the metallicity and dust content increase with decreasing redshift, with [Zn/H]$= -0.56$ (28% solar) and [Cr/Zn]$= -0.64$ at $<z>= 1.15$ and [Zn/H]$= -0.94$ (11% solar) and [Cr/Zn]$= -0.38$ at $<z>= 1.53$. Two explanations, or a combination of the two, seem viable. One is that larger velocity spreads correspond to deeper gravitational potential wells. These more massive regions would lead to more chemically evolved structures. The other is that larger velocity spreads correspond to regions with more intense bursts of star formation. This would also lead to kinematically broad structures of chemically enriched gas.

(4) Finally, the findings presented here suggest that future analyses of the full set of SDSS spectra will result in a significantly better understanding of the neutral-gas-phase metallicity of the Universe in the redshift interval $0.9 \leq z \leq 2.0$, due to the ≈ 30-fold increase in the number of available SDSS spectra and the inclusion of results on weaker Mg II absorbers.

We thank members of the SDSS collaboration who made the SDSS project a success and who made the QSO EDR spectra available.[4] We also acknowledge support from NASA-STScI, NASA-LTSA, and NSF. We thank Eric Furst for initial work on detecting Mg II systems in the SDSS EDR sample of QSOs. DBN thanks Sara Ellison for discussions on searches for dust-reddening in SDSS absorber spectra. This study is an extension of that ongoing work.

[4] Funding for the creation and distribution of the SDSS Archive has been provided by the Alfred P. Sloan Foundation, the Participating Institutions, NASA, NSF, DOE, the Japanese Monbukagakusho, and the Max Planck Society. The SDSS Web site is http://www.sdss.org/. The SDSS is managed by ARC for the Participating Institutions. The Participating Institutions are University of Chicago, Fermilab, Institute for Advanced Study, the Japan Participation Group, Johns Hopkins University, Los Alamos National Laboratory, Max-Planck-Institute for Astronomy, Max-Planck-Institute for Astrophysics, New Mexico State University, University of Pittsburgh, Princeton University, the US Naval Observatory, and University of Washington.

REFERENCES

Ge, J., Bechtold, J., & Kulkarni, V. 2001, ApJ, 547, L1
Grevesse, N., & Sauval, A. 1998, SSR, 85, 161
Howk, J. C, & Sembach, K. R. 1999, ApJ, 523, L41
Molaro, P., et al. 2000, ApJ, 541, 54
Nestor, D. B., Rao, S. M., Turnshek, D. A., & Furst, E. 2002, in *The IGM/Galaxy Connection* (Boulder), in press (astro-ph/0211293)
Pettini, M., Ellison, S., Steidel, C., & Bowen, D. 1999, ApJ, 510, 576
Prochaska, J. X., & Wolfe, A. M. 1999, ApJS, 121, 369
Rao, S. M., & Turnshek, D. A. 2000, ApJS, 130, 1 (RT2000)
Savage, B. D., & Sembach, K. R. 1996, ARA&A, 34, 279
Schneider, D. P., et al. 2002, AJ, 123, 567
Storrie-Lombardi, L., & Wolfe, A. M. 2000, ApJ, 543, 552
Stoughton, C., et al. 2002, AJ, 123, 485
Turnshek, D. A., Rao, S. M., Ptak, A. F., Griffiths, R. E., & Monier, E. M. 2003, ApJ, 590, 730
York, D., et al. 2000, AJ, 120, 1579